JOC*Article*

Kinetics Study and Theoretical Modeling of the Diels−Alder Reactions of Cyclopentadiene and Cyclohexadiene with Methyl Vinyl Ketone. The Effects of a Novel Organotungsten Catalyst

Yaw-Shien Fu, Shih-Chung Tsai, Chun-Huei Huang, Shih-Yao Yen, Wei-Ping Hu,* and Shuchun Joyce Yu*

Department of Chemistry and Biochemistry, National Chung Cheng University, Min-Hsiung, Chia-Yi, Taiwan 621

chejyy@ccu.edu.tw

Received October 23, 2002

The Diels−Alder reaction rate constants of methyl vinyl ketone with cyclopentadiene and cyclohexadiene in the presence of a novel organotungsten catalyst, $[P(2\text{-py})_3W(CO)(NO)_2]^{2+}$, have been measured experimentally and modeled theoretically at several temperatures. The uncatalyzed systems were also studied for direct comparison. When 0.0022 M of catalyst is present at room temperature, the rate constants were found to be approximately 5.3 and 5300 times higher than the corresponding uncatalyzed reactions for cyclopentadiene and cyclohexadiene systems, respectively. Experimental data suggested that the catalyst reduced the activation energies by 5−10 kcal/mol. However, the preexponential factors showed reduction of more than 3 orders of magnitude upon catalysis due to the entropic effects. The energy barriers and the rate constants of the uncatalyzed systems were accurately modeled by correlated electronic structure and dual-level variational transition state theory calculation. The calculated endo selectivity is in good agreement with the observed product distribution. Theoretical calculation also suggested the catalyzed reactions proceeded in a highly asynchronous or even stepwise fashion.

Introduction

The Lewis acid-catalyzed Diels−Alder (DA) reaction[1] is one of the most powerful synthetic tools for the construction of six-membered ring systems that are essential building subunits for various pharmaceuticals and specialty chemicals. For various DA reactions, Lewis acid catalyst can provide not only rate acceleration but also better selectivity compared with the uncatalyzed systems.[2] However, most conventional Lewis acids are generally employed in large quantities due to their extreme water-sensitivity and their feasibility in product binding. These Lewis acids are sometimes too active that undesired side reactions occur. Thus, the development of alternative strategies that use moisture- and air-stable, low-valent organometallic Lewis acids as catalysts under mild conditions and to retain atom economy is of practical importance. From our previous study,[3] we have demonstrated that the organotungsten complex $[P(2\text{-py})_3W(CO)(NO)_2](BF_4)_2$ (**1**) possesses strong Lewis acidity upon loss of the CO ligand, and the relative Lewis acid strength of **1** is found to be comparable to that of BF_3. In addition, **1**

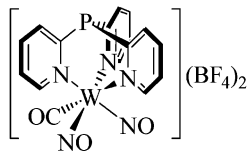

1

can be easily prepared in high yield from $W(CO)_6$, and it can be stored as a crystalline solid in air for months without significant decomposition. In addition, we have also demonstrated that **1** is a potent and selective Lewis acid catalyst for various carbon−carbon formation reactions such as Friedel−Crafts alkylation,[3b] aldehyde cyclotrimerization,[3b] and DA reactions of 1,3-dienes and α,β-unsaturated ketones and/or aldehydes.[3c]

Although numerous new reports on DA reactions are published in the literature each year, there are relatively

* To whom correspondence should be addressed. Fax: (886) 5-272-1040.

(1) (a) Carruthers, W. *Cycloaddition Reactions in Organic Synthesis*; Pergamon Press: Oxford, 1990; pp 50−53. (b) Fringuelli, F.; Tatichi, A. *Dienes in the Diels−Alder Reactions*; Wiley: New York, 1990. (c) Oppolzer, W. *Comprehensive Organic Synthesis*; Fleming, I., Trost, B. M., Eds.; Pergamon Press: Oxford, 1991; Vol. 5, pp 315−399. (d) Roush, W. R. In *Comprehensive Organic Synthesis*; Fleming, I., Trost, B. M., Eds.; Pergamon Press: Oxford, 1991; Vol. 5, pp 513−550. (e) Santelli, M.; Pons, J.-M. *Lewis Acids and Selectivity in Organic Synthesis*; CRC Press: Boca Raton, 1996. (f) H. Yamamoto *Lewis Acids in Organic Synthesis*; Wiley-VCH: Weinheim, 2000.

(2) For reviews see: (a) Kagan, H. B.; Riant, O. *Chem. Rev.* **1992**, *92*, 1007. (b) Pindur, U.; Lutz, G.; Otto, C., *Chem. Rev.* **1993**, *93*, 741. (c) Li, C.-J. *Chem. Rev.* **1993**, *93*, 2023. (d) Cativiela, C.; Garcia, J. I.; Mayoral, J. A.; Salvatella, L. *Chem. Soc. Rev.* **1996**, *25*, 209. (d) Mehta, G.; Uma, R *Acc. Chem. Res.* **2000**, *33*, 278. (e) Kumar, A. *Chem. Rev.* **2001**, *101*, 1.

(3) (a) Kuo, C.-Y.; Fuh, Y.-S.; Shiue, J.-Y.; Lee, G.-H.; Peng, S.-M.; Yu, S. J. *J. Organomet. Chem.* **1999**, *588*, 260. (b) Wang, H.-S.; Yu, S. J. *Tetrahedron Lett.* **2002**, *43*, 1051. (c) Kuo, C.-Y.; Fuh, Y.-S.; Chaen, M.-C.; Yu, S. J. *Tetrahedron Lett.* **1999**, *40*, 6451.

10.1021/jo026596l CCC: $25.00
Published on Web 03/12/2003

few detailed kinetics studies,[4−7] especially those that involve catalysis. In this paper, we report a comprehensive kinetics study of both the uncatalyzed and the corresponding organotungsten Lewis acid **1**-catalyzed DA reactions of cyclopentadiene (CP) with methyl vinyl ketone (MVK) and cyclohexadiene (CH) with MVK at several temperatures. In the current study, the reaction mechanism of the catalyzed system is assumed to be

$$\text{MVK} + \text{Cat-CO} \rightarrow \text{Cat}-\text{MVK} + \text{CO} \quad (1)$$

$$\text{diene} + \text{Cat}-\text{MVK} \rightarrow [\text{Cat}-\text{Ts}] \rightarrow \text{Cat}-\text{product} \quad (2)$$

$$\text{MVK} + \text{Cat}-\text{product} \rightarrow \text{product} + \text{Cat}-\text{MVK} \quad (3)$$

and then (2), (3), and so on. The symbol Cat-CO is used as an abbreviation for the catalyst precursor before its loss of CO ligand, and TS is the symbol for the transition state of diene + MVK. Note that step 1 is based on the experimental observation[3a] that the evolution of CO took place upon the addition of organic Lewis bases such as ketones and aldehydes to the solution of catalyst **1**. Step 2 was assumed to be the rate-determining step.

The results of the current kinetic studies would enable us to obtain quantitative information regarding the rate constants, catalyst efficiencies, and various activation parameters, which are extremely important in understanding the action of catalysis.

The current experimental study was further complemented by theoretical dynamics modeling. Theoretical reaction dynamics calculation can often assist experimental study in understanding the nature of the reaction systems. For example, calculation of the transition states or even the reaction pathways can elucidate the detailed reaction mechanism and can, at least qualitatively, explain the branching ratios of the products if multiple reaction pathways are possible. The causes of the temperature dependence and the extents of the solvation effects can also be probed by using modern electronic structure and reaction dynamics methods. Consequently, in addition to the experimental kinetics measurements in the present study, we also performed various electronic structure calculations on the molecules involved in the reactions. Dual-level variational transition state theory calculation[8,9] with multidimensional tunneling correction (VTST/MT)[10] was also carried out to model the observed reaction rate constants. For the catalyzed reactions, simplified model systems were used to assess the changes in the transition-state structures, reaction pathways, and reaction energy barriers accompanied by the action of the catalyst. It is hoped that by combining the results of experimental kinetics measurements and theoretical modeling, one can gain better insight in both the uncatalyzed and the organometallic Lewis acid-catalyzed DA reactions. In the current study, for the computational resource consideration, we chose $[(NH_3)_3W(NO)_2]^{2+}$ as our model catalyst in which the tripodal ligand, $P(2\text{-py})_3$ of catalyst **1**, was replaced by three monodentate NH_3 molecules. This simplification would certainly reduce the reliability of the modeling to some degree. However, the current theoretical study concerns only the primary catalytic effects exerted by the central metal atom. The simplified model does make the semiquantitative theoretical calculation feasible, and important knowledge can be learned from this model system.

Experimental Section

General Methods. Cyclopentadiene was freshly cracked prior to use. Methyl vinyl ketone was dried over KOH and distilled under nitrogen. Cyclohexadiene was also dried and distilled over $NaBH_4$ under nitrogen. Nitromethane was purified over $CaCl_2$ and dried over $CaSO_4$. The organotungsten Lewis acid $[P(2\text{-py})_3W(CO)(NO)_2](BF_4)_2$ (**1**) was prepared by following literature procedures.[3a] Syringe techniques were employed in the transfer of all liquid reactants. ^{1}H NMR spectra for kinetics measurements and product identification were recorded on a 400 MHz NMR spectrometer. A GC/MS spectrometer was used for the determination of the product identities and the endo/exo ratios.

Kinetics. The kinetics was studied in 10 mL of CH_3NO_2 for both the uncatalyzed and **1**-catalyzed reaction systems. To obtain the activation parameters, the kinetics study were conducted at three different temperatures within 0−100 °C range. Three sets of reactant concentrations were applied to study the reaction orders. See the Supporting Information for experimental details.

Computational Methods. (1) Uncatalyzed System. Geometry optimization of the reactants, products, and the transition states of the uncatalyzed system in the gas phase was performed using the Hartree−Fock (HF),[11] B3LYP hybrid density-functional theory,[12] and Møller−Plesset second-order perturbation theory (MP2)[11,13] with a 6-31+G* basis set.[11] Transition states for four possible pathways (endo-cis, endo-trans, exo-cis, and exo-trans) were calculated. For comparison with the catalyzed systems, the LANL2DZ[14] basis set was also

(4) (a) Goldstein, E.; Beno, B.; Houk, K. N. *J. Am. Chem. Soc.* **1996**, *118*, 6036 and references therein. (b) Beno, B. R.; Houk, K. N.; Singleton, D. A. *J. Am. Chem. Soc.* **1996**, *118*, 9984, and references therein. (c) Gugelchuk M. M.; Doherty-Kirby, A. L. *J. Org. Chem.* **1996**, *61*, 3490. (d) Klemm, L. H.; Solomon, W. C.; Tamiz. A. P. *J. Org. Chem.* **1998**, *63*, 6503. (e) Buback, M.; Heiner, T.; Hermans, B.; Kowollik, K.; Kozhushkov, S. I.; de Meijere, A. *Eur. J. Org. Chem.* **1998**, *107*, 7. (f) Otto, S.; Engberts, J. B. F. N.; Kwak, J. C. T. *J. Am. Chem. Soc.* **1998**, *120*, 9517.

(5) For recent reviews, see: (a) Glebov, E. M.; Krishtopa, L. G.; Stepanov, V.; Krasnoperov, L. N. *J. Phys. Chem. A* **2001**, *105*, 9427. (b) Tsuda, A.; Oshima, T. *J. Org. Chem.* **2002**, *67*, 1282.

(6) (a) Otto, S.; Bertoncin, F.; Engberts, J. B. F. N. *J. Am. Chem. Soc.* **1996**, *118*, 7702. (b) Otto, S.; Engberts, J. B. F. N.; Kwak, J. C. K. *J. Am. Chem. Soc.* **1998**, *120*, 9517.

(7) (a) Brunkan, N. M.; White, P. S.; Gagné, M. R. *Organometallics* **2002**, *21*, 1565. (b) Brunkan, N. M.; Gagné, M. R. *Organometallics* **2002**, *21*, 1576.

(8) (a) Hu, W.-P.; Liu, Y.-P.; Truhlar, D. G.,*J. Chem. Soc., Faraday Trans.* **1994**, *90*, 1715. (b) Corchado, J. C.; Espinosa-Garcia, J.; Hu, W.-P.; Rossi, I.; Truhlar, D. G. *J. Phys. Chem.* **1995**, *99*, 687. (c) Chuang, Y.-Y.; Truhlar, D. G. *J. Phys. Chem. A* **1997**, *101*, 3808.

(9) (a) Truhlar, D. G.; Garrett, B. C. *Acc. Chem. Res.* **1980**, *13*, 440. (b) Truhlar, D. G.; Isaacson, A. D.; Garrett, B. C. In *Theory of Chemical Reaction Dynamics*; Baer, M., Ed.; CRC Press: Boca Raton, 1985; Vol. 4, p 65.

(10) (a) Liu, Y.-P.; Lu, D.-H.; Gonzalez-Lafont, A,; Truhlar, D. G.; Garrett, B. C. *J. Am. Chem. Soc.* **1993**, *115*, 7806. (b) Truong, T. N.; Lu, D.-h.; Lynch, G. C.; Liu, Y.-P.; Melissas, V. Lafont, A.; Rai, S. N.; Steckler, R.; Garrett, B. C.; Joseph, T.; Truhlar, D. G. *Comput. Phys. Commun.* **1993**, *75*, 143.

(11) (a) Hehre, W. J.; Radom, L.; Schleyer, P. v. R.; Pople, J. A. *Ab initio Molecular Orbital Theory*: John Wiley & Sons: New York, 1986. (b) Szabo, A.; Ostlund, N. S. *Modern Quantum Chemistry*; McGraw-Hill: New York, 1989.

(12) (a) Becke, A. D. *J. Chem. Phys.* **1993**, *98*, 5648. (b) Stephens, P. J.; Devlin, F. J.; Chabalowski, C. F.; Frisch, M. J. *J. Phys. Chem.* **1994**, *98*, 11623. (c) Stephens, P. J.; Devlin, F. J.; Ashvar, C. S.; Bak, K. L.; Taylor, P. R.; Frisch, M. J. *ACS Symp. Ser.* **1996**, *629*, 105.

(13) Møller, C.; Plesset, M. S. *Phy. Rev.* **1934**, *46*, 616.

(14) (a) Dunning, T. H. Jr.; Hay, P. J. In *Modern Theoretical Chemistry*; Schaefer, H., F., III, Ed.; Plenum: New York, 1976; Vol. 3, p 1. (b) Hay, P. J.; Wadt, W. R. *J. Chem. Phys.* **1985**, *82*, 270. (c) Wadt, W. R.; Hay, P. J. *J. Chem. Phys.* **1985**, *82*, 284. (d) Hay, P. J.; Wadt, W. R. *J. Chem. Phys.* **1985**, *82*, 299.

TABLE 1. Experimental Rate Constants (in cm^3 Molecule^{-1} s^{-1}) of the Diels−Alder Reactions of CP with MVK at Different Temperatures (°C) and Initial Reactant Concentrations (M)

T	[CP]	[MVK]	k_{expt}	k_{calc}[a]
0	1.00	0.50	3.23 ± 0.32[b] (−26)[c]	4.04 (−26)
	1.00	1.00	3.72 ± 0.33 (−26)	
	0.50	1.00	4.01 ± 0.29 (−26)	
29	1.00	0.50	3.64 ± 0.50 (−25)	3.65 (−25)
	0.50	0.50	4.07 ± 0.20 (−25)	
	0.50	1.00	3.89 ± 0.20 (−25)	
50	0.50	0.25	1.40 ± 0.20 (−24)	1.44 (−24)
	0.50	0.50	1.61 ± 0.22 (−24)	
	0.25	0.50	1.32 ± 0.10 (−24)	

[a] From theoretical modeling, see the text and the Supporting Information. [b] Error in 90% confidence limit. [c] 3.23(−26) means 3.23×10^{-26}.

TABLE 2. Experimental Rate Constants (in cm^3 Molecule^{-1} s^{-1}) of the Diels−Alder Reactions of CH with MVK at Different Temperatures (°C) and Initial Reactant Concentrations (M).

T	[CH]	[MVK]	k_{expt}	k_{calc}[a]
80	2.50	1.25	4.32 ± 0.44[b] (−27)[c]	4.83 (−27)
	2.50	2.50	5.09 ± 0.72 (−27)	
	1.25	2.50	4.39 ± 0.41 (−27)	
90	2.50	1.25	9.82 ± 0.50 (−27)	9.70 (−27)
	2.50	2.50	1.04 ± 0.06 (−26)	
	1.25	2.50	9.96 ± 0.68 (−27)	
100	2.50	1.25	1.90 ± 0.21 (−26)	1.88 (−26)
	2.50	2.50	1.98 ± 0.18 (−26)	
	1.25	2.50	1.74 ± 0.16 (−26)	

[a] From theoretical modeling, see the text and the Supporting Information. [b] Error in 90% confidence limit. [c] 4.32(−27) means 4.32×10^{-27}.

TABLE 3. Experimental Rate Constants (in cm^3 Molecule^{-1} s^{-1}) of the 1-Catalyzed[a] Diels−Alder Reactions of CP with MVK at Different Temperatures (°C) and Initial Reactant Concentrations (M)

T	[CP]	[MVK]	k_{expt}	k_{calc}[b]
0	0.20	0.10	4.88 ± 0.21 (−25)	2.65 (−25)
	0.10	0.10	5.05 ± 0.36 (−25)	
	0.10	0.20	4.46 ± 0.44 (−25)	
27	0.10	0.05	1.98 ± 0.06 (−24)	1.77 (−24)
	0.10	0.10	1.94 ± 0.06 (−24)	
	0.05	0.10	1.80 ± 0.12 (−24)	
50	0.10	0.05	4.31 ± 0.31 (−24)	7.08 (−24)
	0.10	0.10	4.27 ± 0.29 (−24)	
	0.05	0.10	4.27 ± 0.45 (−24)	

[a] The concentration of catalyst **1** is 0.0022 M. [b] From theoretical modeling

TABLE 4. Experimental Rate Constants (in cm^3 Molecule^{-1} s^{-1}) of the 1-Catalyzed[a] Diels−Alder Reactions of CH with MVK at Different Temperatures (°C) and Initial Reactant Concentrations (M)

T	[CH]	[MVK]	k_{expt}	k_{calc}[b]
0	0.25	0.50	6.02 ± 0.24 (−26)	3.22 (−26)
	0.25	0.25	5.42 ± 0.37 (−26)	
	0.50	0.25	5.64 ± 0.70 (−26)	
27	0.25	0.50	2.52 ± 0.54 (−25)	2.35 (−25)
	0.25	0.25	2.57 ± 0.32 (−25)	
	0.50	0.25	2.74 ± 0.36 (−25)	
50	0.25	0.50	6.58 ± 0.57 (−25)	1.00 (−24)
	0.25	0.25	6.69 ± 0.52 (−25)	
	0.50	0.25	6.14 ± 0.81 (−25)	

[a] The concentration of catalyst **1** is 0.0022 M. [b] From theoretical modeling

used with the MP2 and B3LYP methods. The counterpoise calculation[15] was performed on the MP2 and B3LYP results to obtain more reliable relative energies. Polarized continuum model (PCM)[16] was used to estimate the solvation energy in nitromethane. Dual-level VTST/MT calculation at the CVT/μOMT level[8,9,17] was performed for the endo-cis pathways to model the experimental reaction rate constants. (The endo-cis pathway is chosen because it is believed to be the dominant pathway in the uncatalyzed systems. In reality, all four pathways contribute to the total rate constants.) A detailed dynamics approach is described in the Supporting Information. The transition states of the CP dimerization reaction were also calculated at the MP2/6-31+G* and B3LYP/6-31+G* levels for comparison.

(2) Catalyzed System. For the catalyzed system, a simpler model catalyst $[(NH_3)_3W(NO)_2]^{2+}$ was used. The solvation is expected to have significant effects on the energies and molecular structures in the charged-catalyzed systems. The geometries of CP, CH, the Cat−MVK complex, and the Cat−TS complex were optimized at the HF/LANL2DZ and B3LYP/LANL2DZ levels including the solvation effects with the Onsager model.[18] Single-point energy calculations at MP2/LANL2DZ and B3LYP/LANL2DZ levels was performed with the Onsager and PCM models at the optimized geometries. The counterpoise correction was also performed on the single-point energies mentioned above. The same reaction dynamics approach was applied to model the experimental reaction rate constants as in the uncatalyzed systems. We further assumed that the role of the catalyst was only to lower the energy barrier and thus the catalyst was not considered explicitly. This assumption was later found to be inadequate as will be discussed in the next section.

Results and Discussion

(1) Experimental Rate Constants. The measured initial rate constants and the estimated errors are shown in Tables 1−4 (see the Supporting Information for details of data analysis). Arrhenius fits to the experimental rate constants for CP/MVK systems are depicted in Figures 1 and 2. (Arrhenius plots for CH/MVK systems are included in the Supporting Information.) In one of our previous studies,[3c] the uncatalyzed DA reaction of CH and MVK proceeded extremely slowly at temperatures below 70 °C. Only less than 5% conversion was detected after 24 h at room temperature, and about 7% conversion was obtained after 6 h at 70 °C. On the other hand, the uncatalyzed DA reaction of CP and MVK was observed to proceed much faster (∼83% in 20 h at room temperature). This is consistent with our current kinetics study as shown in Tables 1 and 2 that the reaction rate

(15) (a) Morokuma, K.; Kitaura, K. In *Chemical Applications of Atomic and Molecular Electronic Potential*; Poltizer, P., Truhlar, D. G., Eds.; Plenum: New York, 1981; p 215. (b) Boys, S. F.; Bernardi, *F. Mol. Phys.* **1970**, *13*, 440.

(16) (a) Miertus, S.; Scrocco, E.; Tomasi, *Chem. Phys.* **1981**, *55*, 117. (b) Miertus, S.; Tomasi, J. *Chem. Phys.* **1982**, *65*, 239. (c) Cossi, M.; Barone, V.; Cammi, R.; Tomasi, J. *Chem. Phys. Lett.* **1996**, *255*, 327.

(17) Huang, C.-H.; You, R.-M.; Lian, P.-Y.; Hu, W.-P. *J. Phys. Chem. A.* **2000**, *104*, 7200.

(18) Wong, M. W.; Frisch M. J.; Widberg, K. B. *J. Am. Chem. Soc.* **1991**, *113*, 4776.

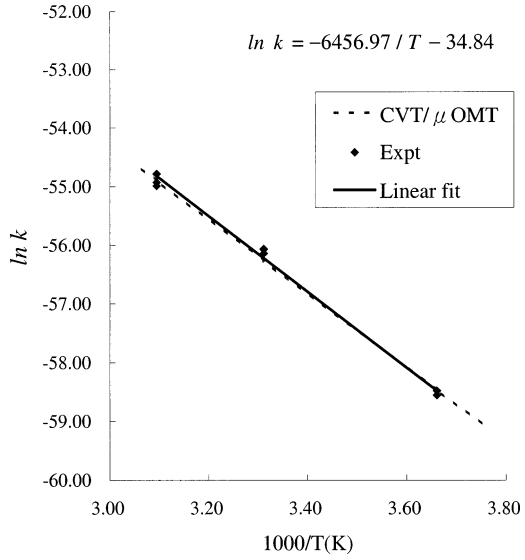

FIGURE 1. Arrhenius plot of the experimental and calculated rate constants (cm^3 $molecule^{-1}$ s^{-1}) of CP with MVK. The solid line is the linear least-squares fit to the experimental values.

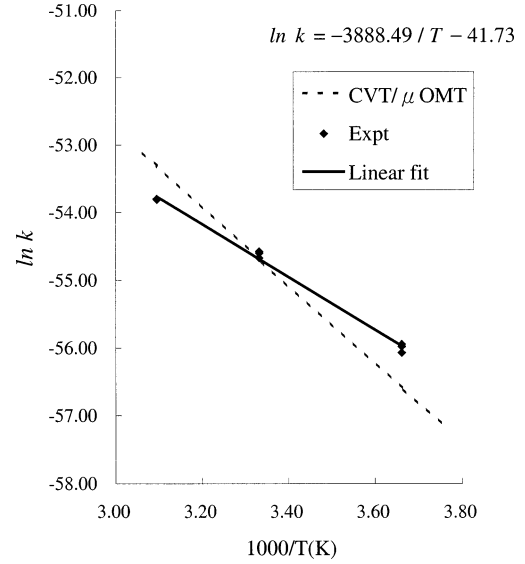

FIGURE 2. Arrhenius plot of the experimental and calculated catalyzed rate constants of CP with MVK.

constant of CP/MVK at 29 °C is about 2 orders of magnitude higher than that of CH/MVK at 80 °C. If the rate constant of the CH/MVK system is extrapolated to 29 °C, it is 7000 times *smaller* than the rate constant of the CP/MVK system. The rate constants of the CP/MVK system have been measured by Breslow et al.[19] in various solvent systems at 293 K. They have shown that the rate constants are very sensitive to the choice of solvents. For example, their rate constant in isooctane is about half of our value obtained in the nitromethane solvent system, while their value measured in methanol is about six times larger than ours.

When 0.0022 M of catalyst **1** is present in the solution, the rate constants at 27 °C were found to be approximately 5.3 and 5300 times higher than the corresponding uncatalyzed CP/MVK and CH/MVK systems, respectively. Under similar conditions, the catalyzed rate constants at 50 °C were found to be 2.9 and 1650 times higher than the corresponding uncatalyzed systems. (The extrapolated rate constants are used for the uncatalyzed CH/MVK reaction system.) The extent of acceleration decreases as the temperature increases, which is as expected when the catalyst lowers the activation energies. The rate constant of the **1**-catalyzed CP/MVK reaction system is only about 10 times higher than that of the **1**-catalyzed CH/MVK system at room temperature. This is also consistent with the earlier observation[3c] that both **1**-catalyzed reactions were found to proceed appreciably within 1 h at temperatures between 0 and 70 °C. Apparently, the catalyst accelerates the slower CH/MVK system more significantly.

The current results can be compared to the recent work by Engbert and co-workers[6] where they studied the DA reactions of 3-phenyl-1-(2-pyridyl)-2-propen-1-ones with CP using 10 mM (∼5 times catalyst loading of the current study) of $Cu(NO_3)_2$ as the catalyst. They observed an ∼30000-fold increase in rate constants in acetonitrile at 25 °C. With the same catalyst loading, our catalyst **1** and Engbert's catalyst is estimated to provide similar rate acceleration in polar organic solvents. Strukul and coworkers[20] have studied the DA reactions of CP and CH with MVK, acrolein, and methacrolein using cationic Pd(II) and Pt(II) complexes as catalysts. They found that with the same dienophile the reaction of CH is much slower than that of CP, which is consistent with our results.

It is well-known that this type of DA reaction can also be accelerated by using solvents such as water and methanol due to the hydrophobic and hydrogen-bonding effects.[19,21,22] However, most of the organic reagents are not soluble in water. In our present study, with the employment of a very low concentration of catalyst **1** (<0.1 mol %), the DA reactions of CH and MVK proceed much more efficiently than in any known solvent systems. For example, when the uncatalyzed DA reactions was carried out in methanol instead of in nitromethane, a 6-fold increase in the rate constant was observed for the CH/MVK system at 50 °C. The difference of the CH/MVK rate constants in the two solvents is consistent with Breslow's results on CP/MVK.[19] However, the rate constant of the **1**-catalyzed DA reaction of CH and MVK at 50 °C is estimated to be 1650 times larger than the corresponding uncatalyzed reaction in nitromethane.

In the **1**-catalyzed systems, the "apparent" rate constants are expected to be proportional to the concentration of the catalyst. This has been carefully checked up in both CP/MVK and CH/MVK systems at three different temperatures by doubling the catalyst concentration from 0.0022 to 0.0044 M. To a good approximation, the bimolecular rate constants thus obtained were all doubled. When the catalyst concentrations were reduced to 0.0011M at 50 °C, we found the rate constants for both CP/MVK

(19) Rideout, D. C.; Breslow, R. *J. Am. Chem. Soc.* **1980**, *102*, 7816.

(20) Pignat, K.; Vallotto, J.; Pinna F.; Strukul, G. *Organometallics* **2000**, *19*, 5160.

(21) (a) Breslow, R. *Acc. Chem. Res.* **1991**, *24*, 159. (b) Breslow, R.; Guo, T. *J. Am. Chem. Soc.* **1988**, *110*, 5613.

(22) (a) Blake, J. F.; Jorgensen, W. L. *J. Am. Chem. Soc.* **1991**, *113*, 7430. (b) Blake, J. F.; Lim, D.; Jorgensen, W. L. *J. Org. Chem.* **1994**, *59*, 803. (b) Furlani, T. R.; Gao, J. *J. Org. Chem.* **1996**, *61*, 5492. (c) Meijer, A.; Otto, S.; Engberts, J. B. F. N. *J. Org. Chem.* **1998**, *63*, 8989.

TABLE 5. Experimental Rate Constants (cm^3 $Molecule^{-1}$ s^{-1}) at Different Catalyst Concentrations[a,b]

	CP + MVK			CH + MVK		
T (°C)	[Cat] = 0.0022 M	[Cat] = 0.0044 M	ratio	[Cat] = 0.0022 M	[Cat] = 0.0044 M	ratio
0	5.05 (−25)	1.01 (−24)	2.00:1	5.42 (−26)	1.25 (−25)	2.31:1
27	1.94 (−24)	3.62 (−24)	1.87:1	2.57 (−25)	5.29 (−25)	2.06:1
50	4.27 (−24)	8.48 (−24)	1.99:1	6.69 (−25)	1.27 (−24)	1.90:1

[a] In the CP/MVK system, the concentrations of the reactants are both 0.100 M; in the CH/MVK system the concentrations of the reactants are both 0.250 M. [b] We have also measured the rate constants with 0.0011 M catalyst at 50 °C. The rate constants are 2.00 (−24) and 3.68 (−25) for the CP/MVK and CH/MVK systems, respectively.

TABLE 6. Experimental Preexponential Factors (cm^3 $Molecule^{-1}$ s^{-1}), Activation Energies (kcal/mol), Activation Enthalpies (kcal/mol), and Activation Entropies (cal/mol K)

	A[a]	E_a[a]	$\Delta^{\ddagger}H°$ (300 K)[b]	$\Delta^{\ddagger}S°$ (300 K)[c]
CP + MVK	7.4×10^{-16}	12.8 ± 0.7[d]	12.2	−130
catalyzed CP + MVK	7.5×10^{-19}	7.7 ± 0.4	7.1	−144
CH + MVK	1.2×10^{-15}	18.4 ± 1.4	17.8	−129
catalyzed CH + MVK	4.2×10^{-19}	8.6 ± 0.4	8.0	−145

[a] From least-squares linear fit to the Arrhenius equation, eq 4 in the text. [b] From eq 5 $\Delta^{\ddagger}H° = E_a - RT$, same uncertainties as E_a. [c] Using eq 5 in the text. [d] Error in 90% confidence limit.

and CH/MVK systems were almost halved. Thus in the range of 1.1 to 4.4 mM of catalyst loading the measured rate constants are indeed proportional to the concentration of the catalyst. These results are shown in Table 5.

(2) Activation Parameters. The Arrhenius plots of the experimental rate constants for the CP/MVK systems are shown in Figures 1 and 2. Each reaction was measured at three different temperatures and three sets of initial concentrations. These nine data points were used to obtain the linear least-squares fits shown in the Figures. Table 6 lists the preexponential factors, activation energies, activation enthalpies, and the activation entropies calculated according to the Arrhenius

$$k = A\mathrm{e}^{-E_a/RT} \tag{4}$$

and Eyring equations.[23]

$$k = e\frac{k_B T}{h}e^{\Delta^{\ddagger}S°/R}\mathrm{e}^{-E_a/RT} = \frac{k_B T}{h}\mathrm{e}^{\Delta^{\ddagger}S°/R}\mathrm{e}^{-\Delta^{\ddagger}H°/RT} \tag{5}$$

For the uncatalyzed systems, the observed activation energies are 12.8 and 18.4 kcal/mol for the CP/MVK and CH/MVK reactions, respectively. As also seen in Table 6, the catalyst lowers the activation energy by approximately 5 kcal/mol for the CP/MVK system and 10 kcal/mol for the CH/MVK system. However, 5−10 kcal/mol of reduction in the activation energy suggests much larger increases in the reaction rate constants than those that were experimentally observed. As seen in Table 6, along with the reduction in activation energies, there are also dramatic decreases (3−4 orders of magnitude) in the preexponential factors, and this corresponds to an approximately 14−16 cal/mol·K reduction in the standard activation entropies. Hence, the DA catalysis by **1** is suppressed by the unfavorable change in the activation entropy. Since the **1**-catalyzed reactions require very specific spatial arrangement between the two reactants and the bulky catalyst in the transition state, the current results are reasonable.

(23) Laidler, K. J. In *Chemical Kinetics*; Harper & Row: New York, 1987; p 114.

TABLE 7. Calculated DA Reaction Energies[a] (kcal/mol).

	CP + MVK		CH + MVK	
	endo	exo	endo	exo
HF/6-31+G*	−14.2	−17.2	−22.5	−22.8
MP2/6-31+G*[b]	−16.9	−18.8	−24.8	−25.0
B3LYP/6-31+G*	−14.3	−16.5	−22.5	−22.7

[a] Born−Oppenheimer energy, not including ZPE, relative to the *trans*-MVK and the diene. [b] Including counterpoise correction for basis set superposition errors (BSSE).

(3) Endo-Exo Selectivity. On the basis of the NMR spectra of the products from the CP/MVK systems, the majority of the DA product was identified as in the endo form, and the endo/exo ratios were apparently enhanced in the catalyzed system. However, for both the uncatalyzed and catalyzed CH/MVK systems, the endo form is the only detectable product from the NMR spectroscopic analysis. Precise endo/exo product ratios were subsequently obtained for both the uncatalyzed and catalyzed CP/MVK systems at three temperatures by GC/MS techniques. For the uncatalyzed system, the product was found to contain 93.0%, 91.0%, and 87.2% of the endo form at 0, 29, and 50 °C, respectively. These ratios were consistent with the integration ratios obtained from the NMR spectra. For the catalyzed system, the endo distributions are 99.2%, 98.5%, and 95.8% at 0, 27, and 50 °C, respectively. That is, the endo selectivity is approximately 6−8% *higher* for the catalyzed system. These product ratios translate approximately to 1.2−1.4 kcal/mol and 2.0−2.6 kcal/mol in the endo-exo activation energy differences for the uncatalyzed and catalyzed systems, respectively. For the CH/MVK systems, we were not able to further resolve the endo/exo ratios by the GC/MS methods, presumably because there was only insignificant amount of *exo* product. This is also consistent with the large endo/exo selectivity in the CH/MVK system obtained from theoretical modeling as will be discussed later in this section.

(4) Theoretical Modeling. (i) Uncatalyzed Systems. Energetics. Table 7 lists the calculated reaction energies in the gas phase at various levels of theory. All energies are relative to the reactants CP or CH and *s-trans*-MVK. All calculations predicted very exoergic reactions. For the CP/MVK system, the *exo*-DA product was found to be more stable by 2−3 kcal/mol while for the CH/MVK system both *endo*- and *exo*-DA products were predicted to be very similar in energies. At the MP2 level, the CH/MVK reaction was predicted to be 6−8 kcal/mol more exoergic than the CP/MVK system. Tables 8 and 9 show the calculated barrier heights at various levels in the gas phase and in nitromethane. The HF/6-31+G* method predicted very high energy barriers while the corresponding MP2 and B3LYP values with the same basis set are lower by more than 20 kcal/mol. It is known that the electron correlation is very important for calcu-

TABLE 8. Calculated Energy Barriers[a] (kcal/mol) of the Diels−Alder Reactions between CP and MVK.

	gas phase				PCM in CH_3NO_2			
	endo-cis	endo-trans	exo-cis	exo-trans	endo-cis	endo-trans	exo-cis	exo-trans
HF/6-31+G*	36.6	39.2	37.2	41.6				
B3LYP/LANL2DZ	18.4	21.6	18.1	23.1	17.3	19.3	17.3	21.2
MP2/LANL2DZ//B3LYP/LANL2DZ	21.0	22.5	21.0	24.6	20.5	20.9	20.3	23.2
	(22.7)[b]	(24.4)	(22.8)	(26.4)	(22.2)	(22.8)	(22.2)	(25.0)
MP2/6-31+G*	10.2	12.8	10.8	15.1	9.8	11.0	10.4	13.7
	(12.1)[c]	(14.9)	(12.9)	(17.1)	(11.8)	(13.1)	(12.5)	(15.7)
B3LYP/6-31+G*	17.4	20.3	17.5	21.8	16.3	18.1	16.9	19.9
	(19.3)[c]	(22.4)	(19.5)	(23.8)	(18.2)	(20.2)	(18.9)	(21.9)

[a] Born−Oppenheimer energy, not including ZPE. The MP2 and B3LYP results include the counterpoise correction for BSSE. [b] Including unscaled ZPE calculated at B3LYP/LANL2DZ level. [c] Including unscaled ZPE calculated at B3LYP/6-31+G* level.

TABLE 9. Calculated Energy Barriers[a] (kcal/mol) of the Diels−Alder Reactions between CH and MVK

	gas phase				PCM in CH_3NO_2			
	endo-cis	endo-trans	exo-cis	exo-trans	endo-cis	endo-trans	exo-cis	exo-trans
HF/6-31+G*	44.1	46.1	45.8	49.3				
B3LYP/LANL2DZ	22.4	25.3	23.2	27.5	21.6	23.6	23.5	26.2
MP2/LANL2DZ//B3LYP/LANL2DZ	24.8	25.6	26.0	28.0	24.4	24.3	26.2	27.1
	(26.3)[b]	(27.2)	(27.5)	(29.7)	(25.9)	(26.0)	(27.7)	(28.8)
MP2/6-31+G*	16.0	18.5	17.9	21.0	17.1	18.9	19.7	22.1
	(17.7)[c]	(20.4)	(19.6)	(22.9)	(18.8)	(20.8)	(21.4)	(24.0)
B3LYP/6-31+G*	22.3	24.7	23.2	27.1	21.3	23.2	23.0	26.0
	(24.0)[c]	(26.6)	(25.0)	(29.0)	(23.1)	(25.1)	(24.8)	(27.9)

[a] Born−Oppenheimer energy, not including ZPE. The MP2 and B3LYP results include the counterpoise correction for BSSE. [b] Including unscaled ZPE calculated at B3LYP/LANL2DZ level. [c] Including unscaled ZPE calculated at B3LYP/6-31+G* level.

lating the energy barriers of DA reactions.[24] All the calculations with the 6-31+G* basis set predicted that the endo-cis pathways have the lowest energy barriers. The barriers calculated in the current MP2/6-31+G* calculation for the CP/MVK system are slightly higher (0.2−1 kcal/mol) than the MP2/6-31G* values reported by Jorgensen et al.[25] Furthermore, in the gas phase, the inclusion of diffuse functions on the heavy atoms increases the energy difference between the endo-cis and exo-cis transition states from 0.29 kcal/mol[25] to 0.64 kcal/mol in the CP/MVK system. The MP2/6-31+G* calculation predicted endo-cis barriers (including vibrational zero-point energies) of 11.8 and 18.8 kcal/mol in nitromethane for CP/MVK and CH/MVK systems, respectively. These values are in good agreement with the experimental activation energies shown in Table 6. The B3LYP method predicted 4−6 kcal/mol higher barriers and similar (∼0.7 kcal/mol) endo selectivity. This is compared to the experimentally estimated (by GC/MS data) 1.2−1.4 kcal/mol endo selectivity for the CP/MVK system mentioned above. The calculated endo selectivity for the CH/MVK system by the MP2/6-31+G* method is ∼2 kcal/mol higher than the CP/MVK system. This is consistent with the experimental result that essentially the entire product is in the endo form. As also seen in Tables 8 and 9, within the polarized continuum model, the effect of solvation is not significant in the uncatalyzed reaction, with changes in barrier heights of approximately 0−2 kcal/mol. However, it should be realized that experimental results have shown that the reaction rate constants in many cases correlate positively with polarity of the solvents.[2d,3c,21b] That is, the solvents can indeed modify the energy barriers to some extent. The specific interaction between the polar solvent molecules and the reacting systems cannot be accurately modeled by the continuum methods such as PCM. Under the experimental conditions, CP may undergo self-dimerization reaction. The calculated gas-phase barrier heights (not including the vibrational zero-point energies) for CP dimerization are 12.2 and 16.8 kcal/mol at MP2/6-31+G* level and are 21.1 and 24.5 kcal/mol at the B3LYP/6-31+G* level for the endo and exo pathways, respectively. That is, the barrier of the endo dimerization pathway is ∼2 kcal/mol higher than the endo-cis pathway for the DA reaction of CP with MVK. Similar results have been reported by Jorgensen et al.[25] This is also consistent with the current experimental results that no detectable amount of dimerization product was observed.

Structures. The calculated transition state structures are depicted in Figures 3 and 4. Table 10 lists the calculated bond lengths of the two forming C−C bonds of the uncatalyzed transition states at various levels. It can be seen that the bond formations are all asynchronous, which is as expected for the unsymmetrical dienophile (MVK). In all cases, the bond connecting the diene and the terminal olefinic carbon of MVK is predicted to form earlier. The bond formations of the endo-cis and exo-cis transition states are the most asynchronous. This is consistent with several earlier studies.[25−29] The MP2/6-31+G* method predicted bond lengths of 2.149 and 2.522 Å for the forming C−C bonds in the endo-cis TS of the

(24) (a) Houk, K. N.; Gonzalez, J.; Li, Y. *Acc. Chem. Res.* **1995**, *28*, 81. (b) Huang, C.-H.; Tsai, L.-C.; Hu, W.-P. *J. Phys. Chem. A* **2001**, *105*, 9945.

(25) Jorgensen, W. J.; Lim, D. L.; Blake, J. F. *J. Am. Chem. Soc.* **1993**, *115*, 2936.

(26) Houk, K. N.; Loncharich, R. J.; Blake, J. F.; Jorgensen W. L. *J. Am. Chem. Soc.* **1989**, *111*, 9172.

(27) Birney, D. M.; Houk, K. N. *J. Am. Chem. Soc.* **1990**, *112*, 4127.

(28) García, J. I.; Martínez-Merino, V.; Mayoral, J. A.; Salvatella, L. *J. Am. Chem. Soc.* **1998**, *120*, 2415.

(29) Avalos, M.; Rabiano, R.; Bravo, J. L.; Cintas, P.; Jiménez, J. L.; Palacios, J. C.; Silva, M. A. *J. Org. Chem.* **2000**, *65*, 6613.

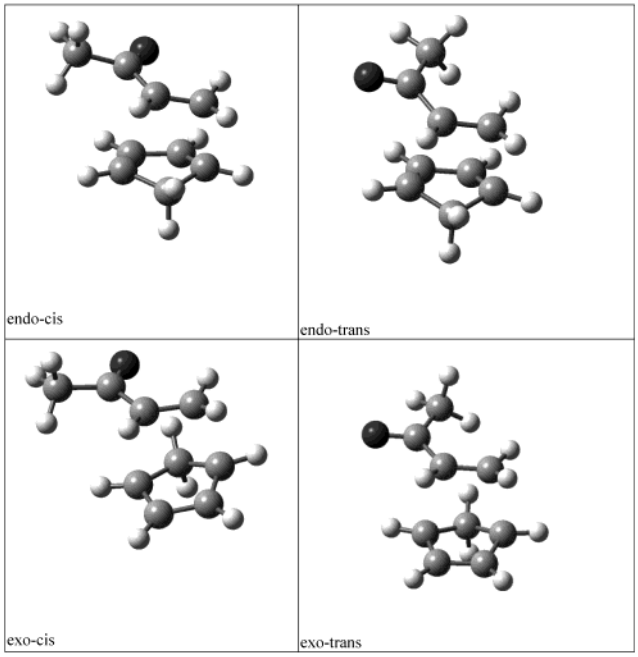

FIGURE 3. Transition-state structures of CP + MVK.

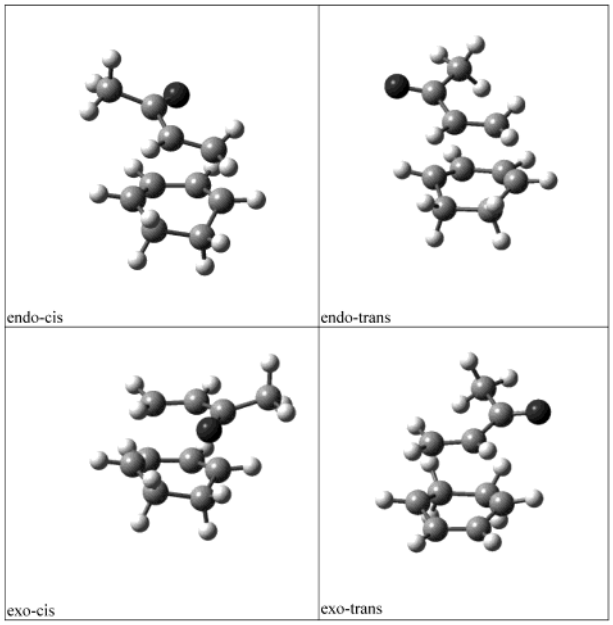

FIGURE 4. Transition-state structures of CH + MVK.

CP/MVK system and 2.152 and 2.596 Å for the CH/MVK system. These values are compared to 2.279 Å for the parent DA reaction (1,3-butadiene + ethylene) calculated at the same level of theory.[24b] The B3LYP method predicted even more asynchronous TS structures in all cases.

Rate Constants. In the theoretical modeling, the classical barrier heights were adjusted to reproduce the experimental rate constants for the CP/MVK system at 29 °C and for the CH/MVK systems at 90 °C. The barriers thus determined plus the zero-point energies are 13.1 and 17.9 kcal/mol for the CP/MVK and CH/MVK systems, respectively. These values are in very good agreement with the experimental activation energies (12.8 and 18.4 kcal/mol) and with the MP2/6-31+G* results (11.8 and 18.8 kcal/mol). That is, a good fit to the experimental rate constants can be achieved by merely adjusting the calculated barrier height by 1.3 and 0.9 kcal/mol for CP/MVK and CH/MVK systems, respectively. There were only negligible variational effects[9] at all temperatures. However, we found that the tunneling effects increase the rate constants by 63% and 70% at room temperatures for the CP/MVK and CH/MVK systems, respectively. Here the tunneling means that the whole system tunnels through a potential energy barrier (from the reactant side to the product side) between two isoenergetic geometries along the reaction path. The geometry changes (or tunneling coordinates) are dominated by the two forming C−C bonds. Even through carbon atoms are relatively heavy; however, the high barriers of the DA reactions make the tunneling effects not negligible at and below room temperature. It can be clearly seen in the Arrhenius plots that even though the rate constants were fitted to a single temperature, the experimental temperature dependence was precisely modeled by the dual-level dynamics calculation.

TABLE 10. Calculated Bond Lengths (Å) of the Forming C−C Bonds in the TS of the Uncatalyzed Reactions[a]

	CP + MVK	
	MP2/6-31+G*	B3LYP/6-31+G*
endo-cis	2.149, 2.522	1.990, 2.690
endo-trans	2.179, 2.358	2.070, 2.430
exo-cis	2.162, 2.464	2.020, 2.580
exo-trans	2.168, 2.381	2.066, 2.460
	CH + MVK	
	MP2/6-31+G*	B3LYP/6-31+G*
endo-cis	2.152, 2.596	2.007, 2.720
endo-trans	2.207, 2.448	2.101, 2.490
exo-cis	2.182, 2.554	2.020, 2.730
exo-trans	2.219, 2.437	2.100, 2.501

[a] The HF/6-31+G* and B3LYP/LANL2DZ results are included in the Supporting Information.

It can be seen from Tables 6, 8, and 9 that the large difference in reactivity between CP and CH is due to the 6−7 kcal/mol difference in reaction energy barrier. We noted that the activation energies of the uncatalyzed CP/MVK and CH/MVK systems are significantly lower than that of the parent DA reactions (27.5 kcal/mol).[24] Both the nature of the dienophiles and the magnitude of the ring strains of the cyclic dienes play important roles in the reduction of the DA energy barriers. Thus, one possible explanation to the difference in the energy barriers between the two systems is that CP is a more strained molecule than CH, and thus in the CP/MVK system the energy of the reactants is closer to that of the DA transition state. For the DA products in the current study, in addition to the six-membered ring formed by the [4 + 2] cycloaddition, another five-membered (for CP/MVK) or six-membered (for CH/MVK) ring is also formed at the same time. The more exoergic CH/MVK reaction (see Table 7) implies that, if everything else being equal, the formation of the new six-membered ring releases 6−8 kcal/mol more energy than the five-membered ring. This is also consistent with the above explanation.

TABLE 11. Calculated Energy Barriers[a] (in kcal/mol) of the Catalyzed Reaction of CP and MVK

	solvation = PCM[b]			
	endo-cis	endo-trans	exo-cis	exo-trans
HF/LANL2DZ	15.3	13.4	10.5	12.6
B3LYP/LANL2DZ	2.0	3.0	3.7	2.4
	(3.7)[c]	(4.8)	(5.4)	(4.0)
MP2/LANL2DZ//B3LYP/LANL2DZ	8.2	11.2	10.2	11.0
	(9.9)[c]	(13.0)	(11.8)	(12.6)

[a] Born−Oppenheimer energy, not including ZPE. The MP2 and B3LYP results include the counterpoise correction for BSSE. [b] The results using the Onsager solvation model are included in the Supporting Information. [c] Including ZPE calculated at B3LYP/LANL2DZ level.

TABLE 12. Calculated Energy Barriers[a] (in kcal/mol) of the Catalyzed Reaction of CH and MVK

	solvation = PCM[b]			
	endo-cis	endo-trans	exo-cis	exo-trans
HF/LANL2DZ	18.3	16.0	13.9	18.2
B3LYP/LANL2DZ	6.0	4.4	7.2	6.0
	(7.7)[c]	(5.9)	(8.6)	(7.4)
MP2/LANL2DZ//B3LYP/LANL2DZ	15.5	14.3	19.6	18.6
	(17.2)[c]	(15.8)	(21.0)	(20.1)

[a] Born−Oppenheimer energy, not including ZPE. The MP2 and B3LYP results include the counterpoise correction for BSSE. [b] The results using the Onsager solvation model are included in the Supporting Information. [c] Including ZPE calculated at B3LYP/LANL2DZ level.

(ii) Catalyzed Systems. Energetics. Even with the simplified model catalyst, modeling the catalyzed systems is very challenging due to their large sizes. Tables 11 and 12 show the calculated energy barriers for the catalyzed systems. Here, the barrier is defined as the difference between the energy of the Cat−TS and the sum of the energies of Cat−MVK complex and the diene. Due to the much larger sizes of the catalyzed systems, the smaller LANL2DZ basis set was used in the geometry optimization instead of the 6-31+G* set used in the uncatalyzed systems.

We found that the Onsager solvation model significantly underestimated the energy barriers while the PCM model predicted more reasonable barrier heights. Thus, the following discussion will be based on the PCM results. For the CP/MVK system, at the MP2 level (B3LYP/LANL2DZ geometry) the endo-cis pathway was found to have the lowest barrier of 9.9 kcal/mol that is about 2 kcal/mol higher than the experimental activation energy. The calculated endo selectivity (∼2.0 kcal/mol) at the MP2 level is in good agreement with the experimentally estimated value of 2.0−2.6 kcal/mol mentioned earlier in this section. The B3LYP calculation also predicted endo-cis to be the lowest energy pathway but with barriers approximately 4 kcal/mol too low and a very small endo selectivity (0.3 kcal/mol). For the CH/MVK system, at the MP2 level the endo-trans pathway was found to be the one with the lowest barrier of 15.8 kcal/mol that is about 7 kcal/mol higher than the experimental activation energy. The calculated endo selectivity is 4.3 kcal/mol at the MP2 level. The high endo selectivity is also consistent with the results obtained from both the NMR and GC/MS analyses. The B3LYP calculation also predicted endo-trans to be the lowest energy pathway but with barriers approximately 3 kcal/mol too low and a smaller endo selectivity (1.6 kcal/mol). The overestimation of the barriers by the MP2 calculation is expected because of the lower quality of the atomic basis set applied compared to the uncatalyzed systems. At the MP2/LANL2DZ (PCM) level, the barrier reduction by the catalysis was calculated to be 10−12 kcal/mol while the experimental activation energies showed a reduction of 6−10 kcal/mol. At the MP2 level the endo selectivity was calculated to be significantly higher (1−2 kcal/mol) than that of the uncatalyzed systems, which is consistent with the current experimental results for the CP/MVK system.

Interestingly, in the current systems the combined effects of the organotungsten Lewis acid catalyst and solvation on the energy barrier reduction (∼10 kcal/mol) were found to be similar to earlier experimental and theoretical results on the Diels−Alder reactions catalyzed by simple Lewis acids such as BH_3, BF_3, and $AlCl_3$.[27−30]

Structures. The calculated structures of the Cat−TS are depicted in Figures 5 and 6 and the calculated bond lengths of the two forming C−C bonds are shown in Table 13. In some cases, for a particular pathway more than one TS differing on the relative orientations between the model catalyst and the diene/MVK units were found. Their energies are all within 2 kcal/mol. Only the one with the lowest energy is considered here. Note that the bond lengths of the two forming C−C bonds in the TS are now significantly different. In particular, at the B3LYP/LANL2DZ level the differences between the two bond lengths are 1.1−1.2 Å in the CP/MVK system and are 1.4−2.2 Å in the CH/MVK system. These are compared with the 0.2−0.4 and 0.4−0.9 Å differences in the uncatalyzed systems predicted by MP2/6-31+G* and B3LYP/LANL2DZ calculation, respectively. Apparently, in the catalyzed DA reactions the bond formations are much more asynchronous than the uncatalyzed reactions, especially for the CH/MVK system. This raised the question whether the catalyzed reactions might even be stepwise. We were able to locate a second transition state (and the corresponding complex between the two transition states) corresponding to the formation of the second C−C bond at HF/LANL2DZ level in the gas-phase for all four pathways for the CP and CH systems. The calculated structure of the second TS for the endo-cis pathway of

(30) Inukai, T.; Kojima, T.; *J. Org. Chem.* **1967**, *32*, 872.

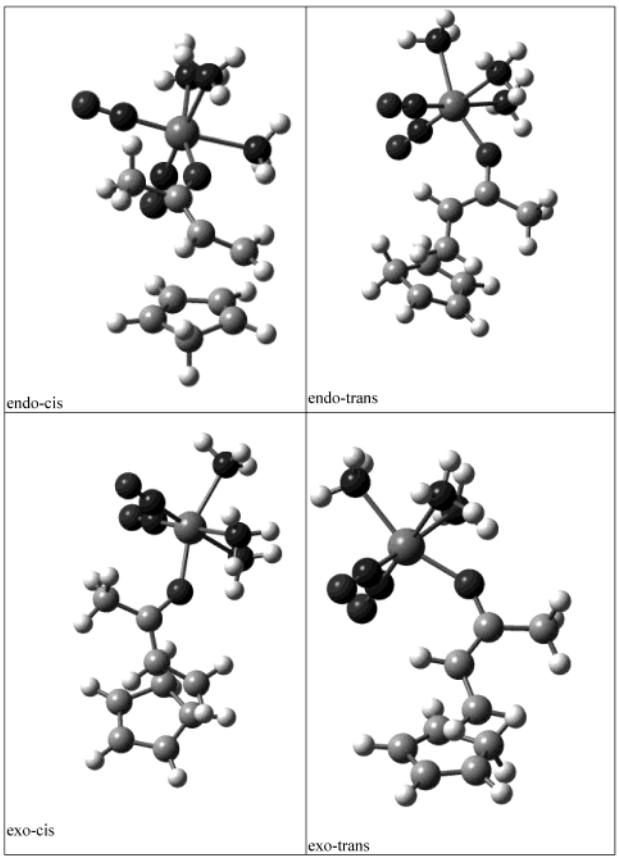

FIGURE 5. Transition-state structures of CP + MVK with the model catalyst.

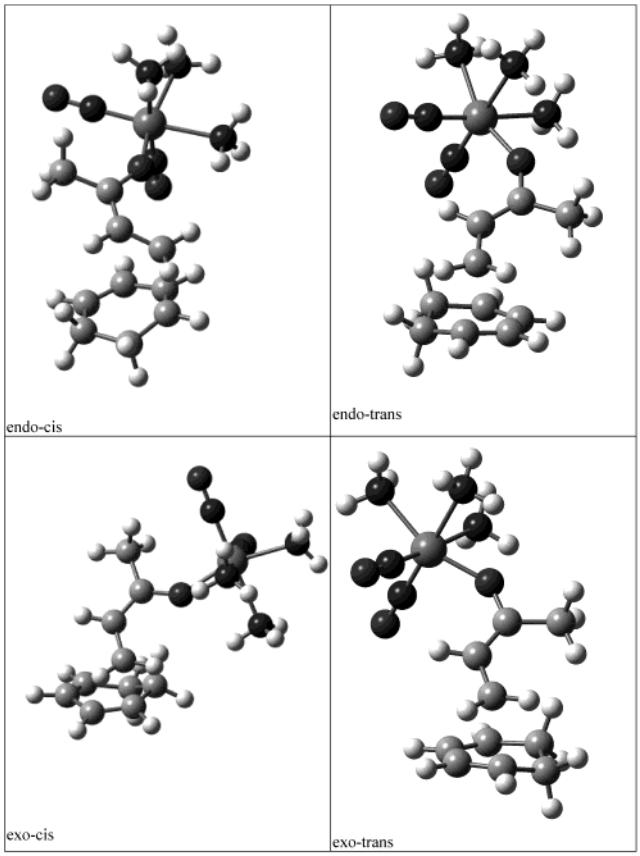

FIGURE 6. Transition-state structures of CH + MVK with the model catalyst.

the CH/MVK system is shown in Figure 7. However, the energies of the second TS are significantly lower than the first TS. For example, in the CP(CH)/MVK system the second TS on the endo-cis pathway is 9.5 (11.6), and 6.0 (11.1) kcal/mol lower than the first TS at the HF/LANL2DZ and MP2/LANL2DZ (PCM) levels, respectively. Thus, even though the second TS implies that the catalyzed reactions might actually be stepwise, the second step would be very fast, and the first step is the rate-determining step. Actually the second TS are only resolvable in the HF calculation. When the correlation energies are included (MP2, B3LYP methods) either in geometry optimization or single point energy calculation, the second TS disappeared. (That is, the energies along the reaction path were found to decrease monotonically from the first TS to the product.) We did not find any low-lying [2 + 4] hetero-DA transition states that are sometimes artifacts of low-level Hartree−Fock calculation.[28,29,31,32] Recent studies by Silva et al.,[33] Tanaka and Kanemasa,[34] and Roberson et al.[35] also suggested that Lewis acid catalyzed cycloaddition reactions might occur through a stepwise mechanism. However, their semiempirical and Hartree−Fock calculation very likely overestimated the energy barriers of the second TS due to the implicit treatment or omission of the electron correlation energies. On the other hand, recent high-level theoretical calculations[36−38] showed that the radical cation DA reactions proceed through stepwise mechanisms. The theoretical study over recent years seem to reach a consensus that most uncatalyzed Diels−Alder reactions with asymmetric diene/dienophile proceed through concerted asynchronous pathways. When the DA reaction is catalyzed by a Lewis acid, the electron density is drawn out of the system and the reaction pathways become

TABLE 13. Calculated[a,b] Bond Lengths (Å) of the Forming C−C Bonds in the TS of the Catalyzed DA Reactions.

	CP + MVK	CH + MVK
endo-cis	(2.115, 3.170)	(2.019, 3.407)
endo-trans	(2.053, 3.143)	(2.094, 3.691)
exo-cis	(2.150, 3.230)	(1.968, 4.167)
exo-trans	(2.050, 3.240)	(1.986, 3.474)

[a] Solvent effects were considered with the Onsager model. [b] Geometry calculated at B3LYP/LANL2DZ level. Results of HF/LANL2DZ level are listed in the Supporting Information.

(31) Yamabe, S.; Dai, T.; Minato, T. *J. Am. Chem. Soc.* **1995**, *117*, 10994.
(32) García, J. I.; Mayoral, J. A.; Salvatella, L. *J. Am. Chem. Soc.* **1996**, *118*, 11680.
(33) (a) Alves, C. N.; Camilo, F. F.; Cruber, J.; Silva, A. B. F. *Tetrahedron* **2001**, *57*, 6877. (b) Alves, C. N.; Silva, A. B. F.; Martí, S.; Moliner, V.; Oliva, M.; Andrés, J.; Domingo, L. R. *Tetrahedron* **2002**, *58*, 2695.
(34) Tanaka, J.; Kanemasa, S. *Tetrahedron* **2001**, *57*, 899.
(35) Roberson, M.; Jepsen, A. S. J.; Jorgensen, K. A. *Tetrahedron* **2001**, *57*, 907.
(36) Haberl, U.; Wiest, O.; Steckhan, E. *J. Am. Chem. Soc.* **1999**, *121*, 6730.
(37) (a) Hofmann, M.; Schaefer, H. F., III. *J. Am. Chem. Soc.* **1999**, *121*, 6719. (b) Hofmann, M.; Schaefer, H. F., III. *J. Phys. Chem. A.* **1999**, *103*, 8895.
(38) Saettel, N.; Wiest, O.; Singleton, D. A.; Meyer, M. P. *J. Am. Chem. Soc.* **2002**, *124*, 11552.

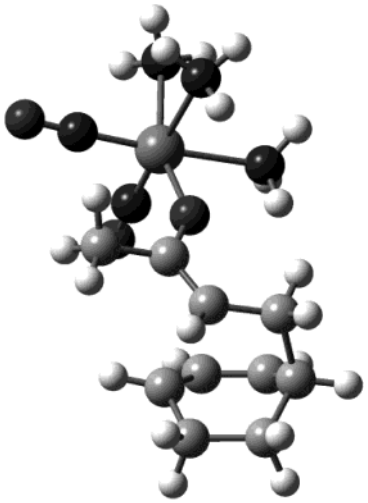

FIGURE 7. Structure of the second endo-cis transition state of the catalyzed CH/MVK system at HF/LANL2DZ level.

highly asynchronous. In the extreme cases of very strong Lewis acid catalysis or in the radical cation DA reactions, the pathways become stepwise.

It is also noted that since in our model systems ammonia molecules were used in place of pyridines in **1**, some additional errors were introduced. For example, the difference in the coordinating strengths to the metal would certainly affect the Lewis acidity of **1** and thus the catalytic efficiency. Also, the $P(2\text{-py})_3$ unit of **1** makes it more rigid than our model catalyst, and this would cause some differences in the structures. In addition, the pyridine is a potential π acid and might further modify the electron density on the metal atom.

Rate Constants. We have also tried to model the experimental rate constants of the catalyzed systems using the dual-level VTST/MT approach. We used the same reaction-path information as in the uncatalyzed systems except adjusting the classical barrier heights to fit the measured rate constants at 27 °C for the CP/MVK and CH/MVK systems. The resulting effective barriers (including the zero-point energies) of 11.8 and 12.4 kcal/mol are approximately 4 kcal/mol too high as compared to the experimental activation energies. The calculated and experimental rate constants of the catalyzed CP/MVK system are plotted in Figure 2. (A figure for the CH/MVK system is in the Supporting Information.) As seen in these figures, the calculated temperature dependence of the rate constants is too large. This clearly demonstrated that it is *inappropriate* to model the catalyzed reaction as just a lower barrier uncatalyzed reaction. The reason for the overestimation of the barrier height or the temperature dependence is because the entropies of activation for the catalyzed reactions are much more negative, as seen in Table 6. As a result, the preexponential factors for the catalyzed reaction are much *smaller* than the uncatalyzed reactions. Thus, a realistic modeling of the catalyzed reaction rates should take the entropic factors into account. Otherwise, the energy barrier and the temperature dependence of the rate constants cannot be modeled accurately.

Summary

Kinetics measurements have been made on the Diels–Alder reactions between methyl vinyl ketone with cyclopentadiene and cyclohexadiene as well as on the same reactions with the presence of an organotungsten Lewis acid catalyst. The catalysis resulted in very significant acceleration, especially for the cyclohexadiene/methyl vinyl ketone system. Theoretical modeling was performed on the uncatalyzed and catalyzed systems and the results are consistent with the experimental activation energies, endo selectivity, the temperature dependence of the uncatalyzed reaction rate constants, and the barrier reductions upon catalysis. The quantitative experimental data and the semiquantitative theoretical modeling information obtained in the current study might be useful for gaining better insights in the transition-metal catalyzed chemical reactions and for future theoretical modeling of catalyzed DA reactions.

Acknowledgment. This research is supported by the National Science Council of Taiwan, Grant Nos. NSC 89-2113-M-194-021 and NSC 88-2113-M-194-018. We are grateful to the National Center for High-Performance Computing of Taiwan for providing part of the computational resources. We would also like to thank Mr. Ming-Cheng Chen and Ms. Li-Chao Tsai for very helpful discussions early in this project.

Supporting Information Available: Detailed description of the experimental conditions/procedures and the dual-level reaction dynamics calculation, Arrhenius plots for the CH/MVK systems, calculated bond lengths and energy barriers, and the Cartesian coordinates and absolute energies of the calculated transition states. This material is available free of charge via the Internet at http://pubs.acs.org.

JO026596L